FILME SUBȚIRI DE PARILENĂ-N ȘI PARILENĂ-C DEPOZITATE PE Si(111) PRIN DEPUNERE POLIMERICĂ DE VAPORI STUDIATE PRIN MICROSCOPIA PRIN FORȚĂ ATOMICĂ ȘI MICROSCOPIA CU BALEIAJ

ATOMIC FORCE MICROSCOPY AND SCANNING ELECTRON MICROSCOPY ON PARYLENE-N AND PARYLENE-C THIN FILMS DEPOSITED ON Si(111) VIA POLYMER VAPOUR DEPOSITION (PVD)

M.A. IONESCU*, I. CIUCĂ
Faculty of Science and Materials Engineering, Politehnica University Bucharest, Romania

Surface roughness measurements by AFM and SEM were performed on thin films of Parylene-N and Parylene-C deposited via Chemical Vapour Deposition of polymers also known as Polymer Vapour Depostion (PVD) on Si(111). AFM revealed a smoother surface for Parylene–C, while the parylene–N showed a dimpled surface with isolated valleys. SEM on Parylene–C showed a smooth surface, with debris, while the Parylene–N revealed a dimpled surface with fibrils bundled together. Angles measured on AFM profile lines are larger when compared to angles measured on SEM images because of the broadening effect in AFM due to tip size. Global features are kept similar. The Parylene-C coating appears with a convex shape, the edges being thicker with a gradient towards the center. Parylene – N appears uniform in thickness with the dimpled aspect observed on the smaller observed surface.

At least at this scale, by surface morphology, we could infer that Parylene – N was deposited homogeneous or that the Parylene – C coating was warped. If this is so we think that Parylene-N's higher level molecular activity during deposition generates greater penetration into crevices than that observed in Parylene-C, making it superior for coating complex topographies specially for medical instrumentation.

Rugozitatea filmelor subțiri de parilenă-N și parilenă -C depuse prin depunere polimerică de vapori pe Si(111) a fost studiată prin microscopie cu forță atomică și microscopie cu baleiaj. Prin microscopie cu forță atomică suprafața filmului subțire de parilenă-C apare mai netedă în comparație cu cea a parilenei-N. Prin microscopie cu baleiaj s-a evidențiat de asemenea pentru parilena-C o suprafață netedă în comparație cu cea a parilenei-C. Unghiurile măsurate prin microscopie cu forță atomică pentru parilena-C au valori mai mari comparativ cu cele măsurate pentru parilena-N. Trăsăturile globale sunt similare pentru cele două filme.

Morfologia suprafețelor arată că filmul de parilenă-N a fost depus într-o manieră omogenă în timp ce cel de parilenă-C a fost depus într-un mod neomogen. Această comportare se poate explica prin faptul că parilena-N prezintă o penetrare mai mare în uniformitățile suprafeței de Si(111) decât parilena-C, generând un strat de protecție superior acoperirilor cu aceasta din urmă în cazul instrumentarului medical.

Keywords: *Atomic Force Microscopy, Scanning Electron Microscopy, Parylene-N, Parylene-C*

1. Introduction

Parylene polymers that are suitable for application ranging from microelectronics to medical industry are deposited onto the substrate via polymer vapour deposition (gas-phase polymerization deposition). On the substrate they form a transparent film with a thickness ranging from fractions of a nanometer (monolayer) to few micrometers. [1]. The Parylene film is conformal, resistant to hostile environment (organic and inorganic reagents), adheres to ceramics, glass, and metal. Its dielectric strength is higher than 5000 V DC / mil of coating thickness [2, 3].

Since the deposition process include no liquid phase the absence of capillarity is fulfilled. Other advantages of Parylene thin films are: conformability, optical clarity, pinhole-free surface, low dielectric constant, zero out-gassing, low static and dynamic coefficients. To the above advantages one should not forget that Parylene thin films are biostable (medical instrumentation covered with Parylene film can be sterilized) and biocompatible making them excellent candidates in prostetics. Parylene-C is a Class VI FDA (Food and Drug Administration – USA) approved polymer (USP XXII – United States Pharmacopoeia - USA) being safe for use within the body, therefore the risk of un-polymerizable monomer which can induce toxic effect is zero.

Our study is centered toward Parylene-C (Fig.1) and Parylene-N (Fig.2). The only structural

* Autor corespondent/*Corresponding author*,
E-mail: mateiionescu@yahoo.com.

difference between the two is a single chlorine (Parylene-C) atom that substitute of one aromatic hydrogen (on Parylene-N) [2, 3]. Parylene-C and Parylene-N were deposited via PVD on Si(111) followed by surface roughness measurements as revealed by atomic force microscopy (AFM).

Fig.1 - Parylene-C [2] / *Parilena-C [2].*

Fig.2 Parylene-N [2] / Parilena-N [2].

2. Experimental details

2.1 PVD of Parylene-N and Parylene-C on Si(111)

Silicon wafers are largely used in microelectronics chip fabrication. Parylene coated surfaces are characterized by a low dielectric constant. The Si wafers (MTI Corporation, Richmond, CA 94804, USA) were a p-Si with B as dopant, orientation <111> ± 0.5°, resistivity 0.7-1.2 Ohm-cm, double-side polished, (5x21 mm^2), thickness 300 µm ± 25 µm.

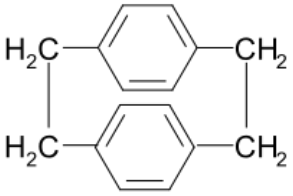

Fig. 3 – Dimer di – para – xylylene / *Dimerul di-para-xililen* [4].

The dimer (di-para-xylylene) (Fig. 3) was purchased from Metal Improvement Company LLC - *Parylene Coating Services - Galway Division*, Ireland. The polymerization onto the substrate was also performed at the above company. The polymerization process is described in detail elsewhere. The surface on which polymerization takes place is pinhole free and the polymer covers it conformally [5].

2.2 Ellipsometry

Parylene-C and Parylene-N film thickness measurements were performed on a Woollam V-VASE ellipsometer. The measurements were performed in the 200–1700nm spectral range at: 45°, 60° and 75°, respectively. The results are presented elsewhere [6].

2.3 Atomic force microscopy

The surface morphology and roughness was examined by recording atomic force microscopy images with an Ntegra Aura scanning probe microscope in contact mode with a commercial DCP20 cantilever.

2.4 Scanning electron microscopy (SEM)

The SEM studies were performed on a FEI Quanta Inspect F using ETD and BSED detectors.

3. Results and discussion

3.1. PVD of Parylene-N and Parylene-C on Si(111)

The Parylene-C thin film deposition a rate was 0.12mil / hour. Parylene-N deposited at lower rate. Mass spectra, pressure and temperature and thickness were monitored during the entire deposition process. Adhesion and dielectric constant measurement have been performed as well.

3.2. Spectroscopic ellipsometry

The thickness of the Parylene-N thin film was 3072 nm, while that of the Parylene-C film was 3777 nm. The Thickness non-uniformity on the wafers was measured as well (+/- 20 nm)[6].

3.3. Atomic force microscopy

The data obtained from the AFM, in ASCII format, was imported and images were reconstructed for processing.

3.3.1. Studies on Parylene – C

For Parylene-C a surface of 100µm^2 (10x10µm) was investigated. The graphs are plotted at first as matrix in grayscale (Fig. 4), a contour plot with color fill (Fig. 5) and a 3D reconstruction of the surface (Fig. 6). On this graphs regions of interest are identified, in this case the presence of a deep valley and a peak surrounded by valleys.

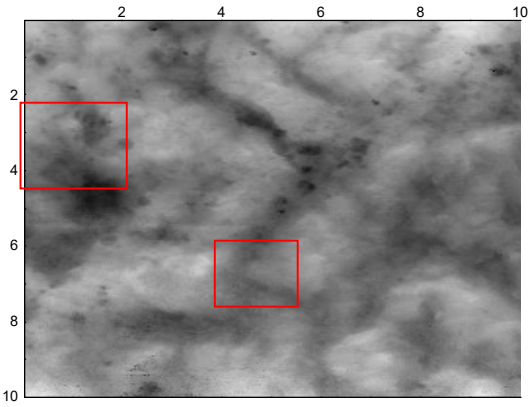

Fig. 4 - Reconstructed image / *Imagine reconstruită.*

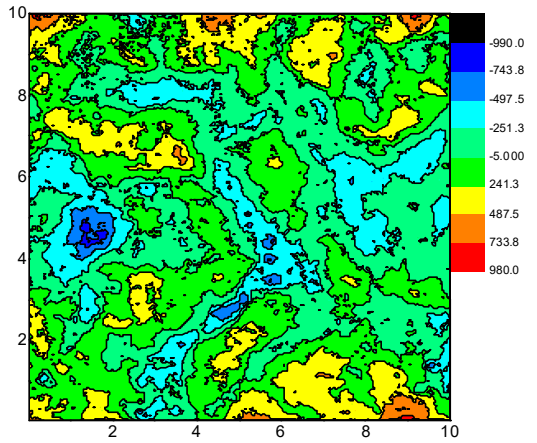

Fig. 5 - Contour plot with color fill / *Conturul trăsăturilor suprafeței.*

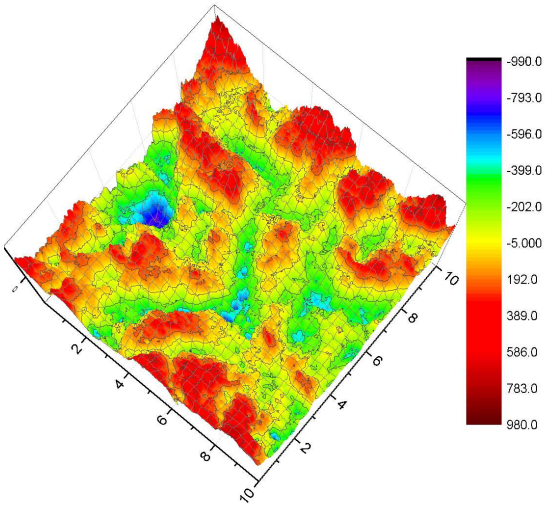

Fig. 6 - 3D reconstruction of the surface / *Reconstrucția 3D a suprafeței.*

The 3D reconstruction of the image, fig. 6, shows an interconnected network of valleys, while deep valleys appear isolated.

A deep valley was observed at coordinates (4.6μm, 1.5 μm) and a chevron shaped valley marked in Figures 4 and 5. These are the lowest regions observable on the investigated surface. By selecting these regions of interest separate graphs depicted by Figures 7 and 8 were constructed to observe the transition from valley to hill.

It appears to be a gradual transition from valley to hill, with intermediate steps.

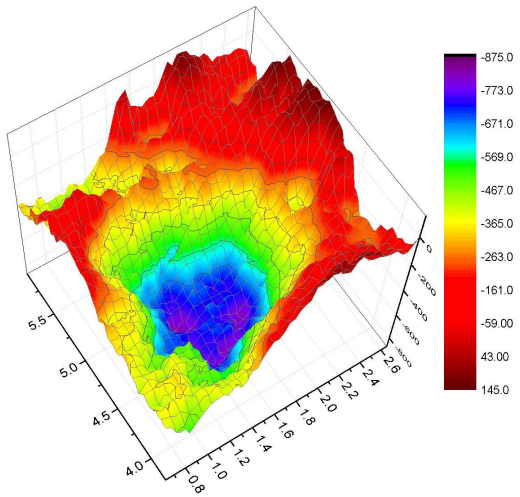

Fig. 7 - Detail of the lowest valley on the surface / *Detaliu pentru cea mai adâncă trăsătură.*

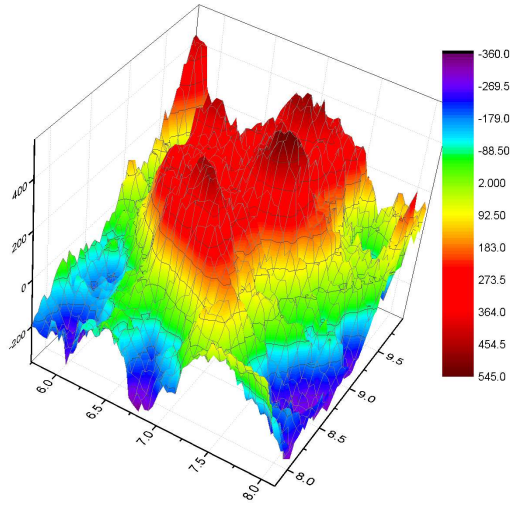

Fig. 8 - Details on a peak surrounded by valleys / *Detaliu pentru un vârf înconjurat de văi.*

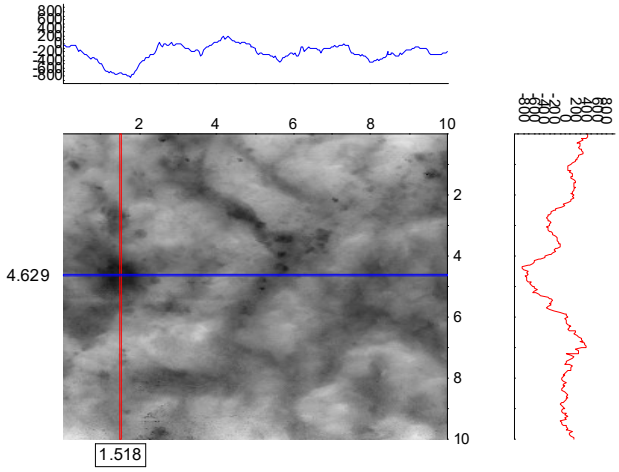

Fig. 9 -Profile lines crossing the deepest valley/ *Liniile de profil pentru cea mai adâncă vale.*

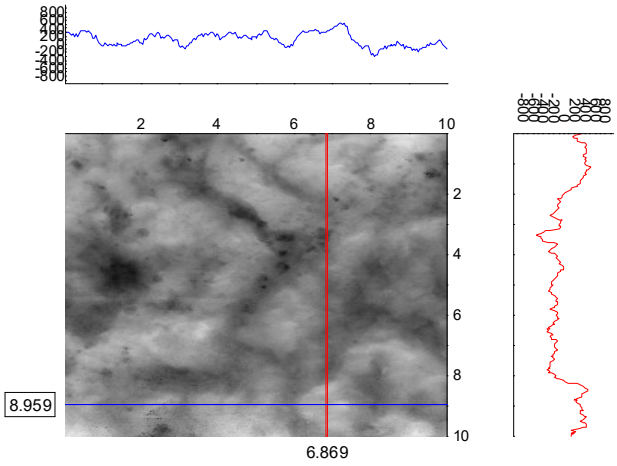

Fig. 10 - Profile lines following peak tops / *Liniile de profil pentru un vârf.*

The profile lines on the deepest valley, fig. 9, show the lowest values at -818nm on the x axis parallel line and -820nm on the y axis parallel line, while the highest values are found at 171nm on the x axis line and 407nm on the y axis line. The ranges, the difference of height between mountain and valley are 647nm on x axis parallel line and 413nm on y axis parallel line.

The profile line on the peak region, fig. 10, presented maximum heights of 527nm on the x axis parallel line and 524nm on the y axis parallel line, while the lowest regions on those lines -277nm (on the x axis parallel line) and -516nm (on the y axis parallel line). The ranges are 250nm and 8nm.

3.3.2 Studies on Parylene – N

The same procedure in processing the obtained data was applied for Parylene-N: plotting the matrix in grayscale, Figure 11, creating a contour plot with color fill, Figure 12, and reconstructing the 3D surface, Figure 13.

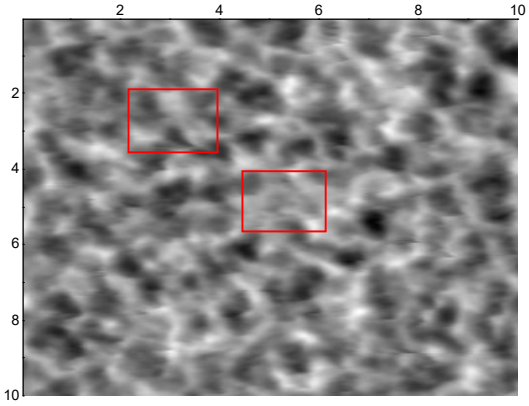

Fig. 11 - Reconstructed image / *Imagine reconstruită.*

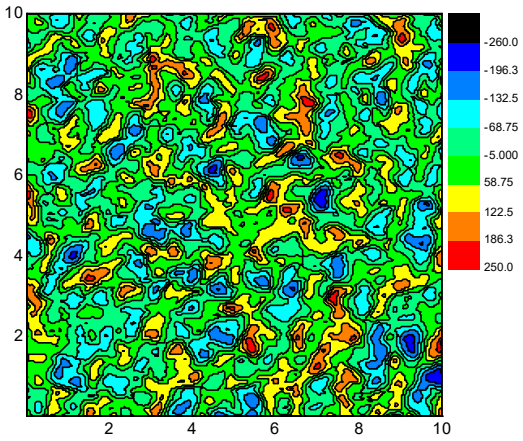

Fig. 12 - Contour plot with color fill. / *Conturul trăsăturilor suprafeței.*

The surface investigated first was 10x10μm. The surface was dimpled, with isolated valleys and hills (Fig. 13). A detailed view of a peak surrounded by valleys (Fig. 14) and a peak surface (Fig. 15) are plotted for better observation.

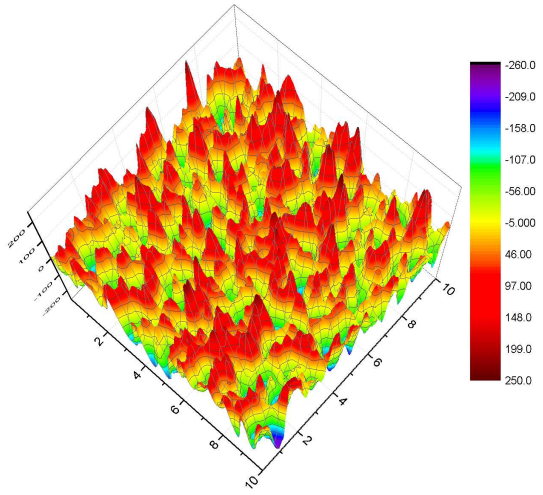

Fig. 13 - 3D reconstruction of the surface / *Reconstrucția 3D a suprafeței.*

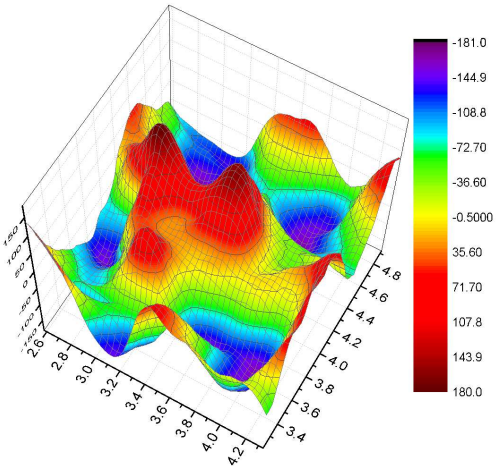

Fig. 14 - Detail of a peak and several valleys / *Detaliu al unui vârf și al unor văi.*

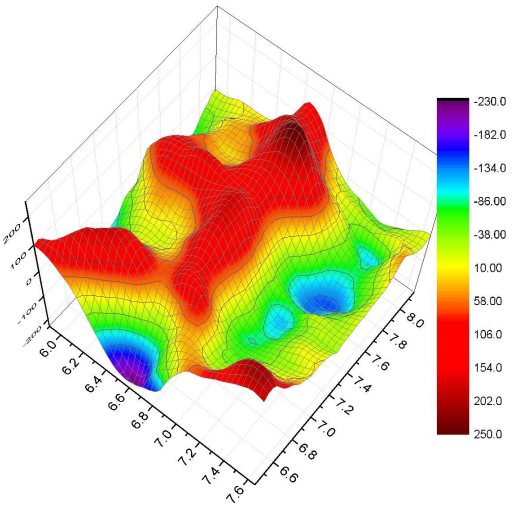

Fig. 15 - Detail of a peak / *Detaliu al unui vârf.*

The valley to hill transition appears to be in stages.

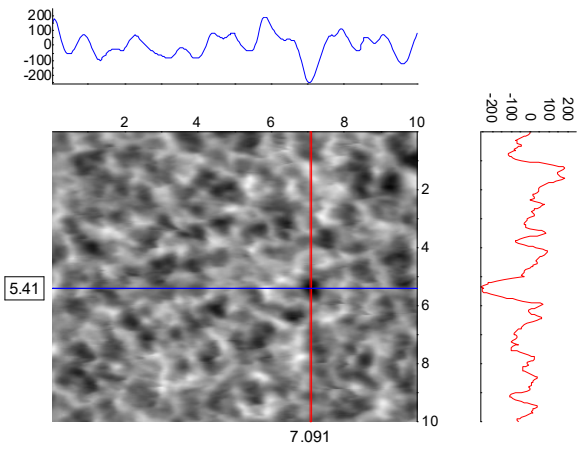

Fig. 16 - Profile lines crossing the deepest valley/ *Liniile de profil pentru cea mai adâncă vale.*

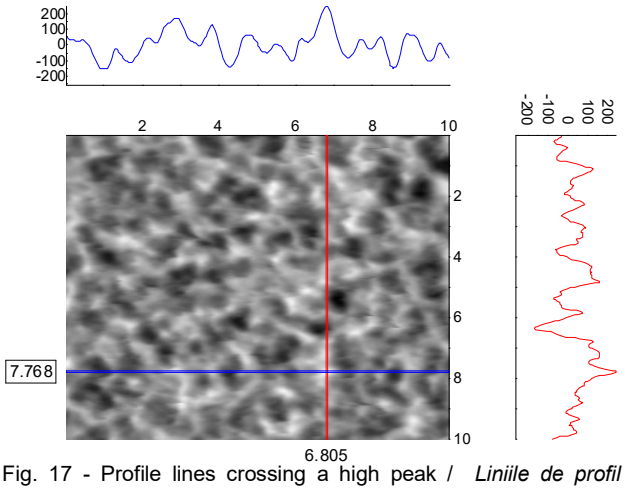

Fig. 17 - Profile lines crossing a high peak / *Liniile de profil pentru un vârf.*

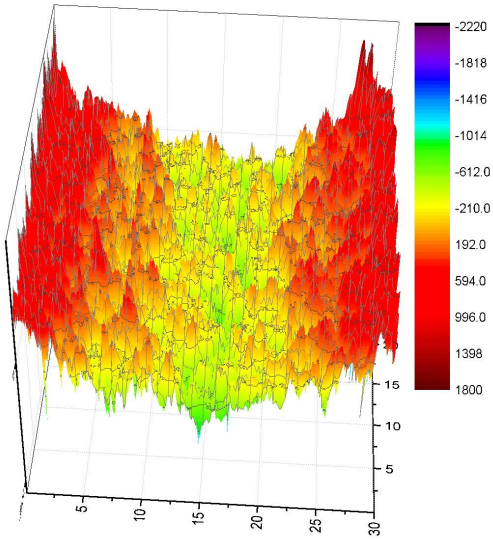

Fig. 18 - Parylene – C on a 30x30µm surface / *O suprafață de 30x30µm a parilenei-C.*

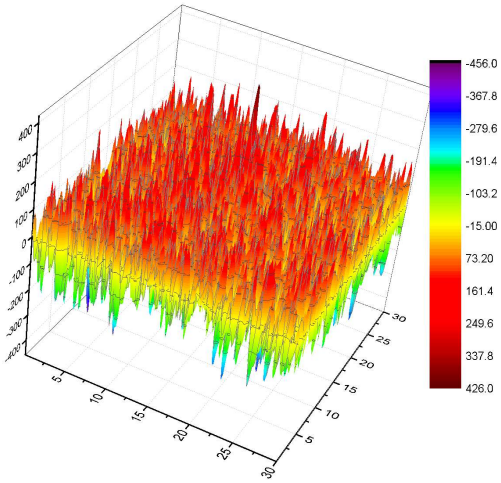

Fig. 19 - Parylene – N on a 30x30µm surface / *O suprafață de 30x30µm a parilenei-N.*

The line profiles from fig. 16 show the highest values at 196nm on the x axis parallel line and 185nm on the y axis parallel line while the lowest values at -254nm on the x axis parallel line and -260nm on the y axis parallel line in the valley region. The range, mountain to valley difference can be calculated at 58nm and 75nm.

On a peak region by inspecting profile lines shown in fig. 17 the highest point on the mountain was found and 249nm on the x and y axis parallel line while the lowest point on the profile line was found at -156nm on the x axis parallel line and -168nm on the y axis parallel line. The range was computed to be 93nm and 81nm.

A scan on an increased surface, 30x30µm surface for both Parylene – C revealed and Parylene – N was performed. In Figures 18 and 19 the reconstructed 3D surface was plotted.

The Parylene – C coating appears with a convex shape, the edges being thicker with a gradient towards the center. Parylene – N appears uniform in thickness with the dimpled aspect observed on the smaller observed surface.

At least at this scale, by surface morphology, we could infer that Parylene – N was deposited homogeneous or that the Parylene – C coating was warped.

3.4. SEM studies

The SEM images revealed a smoother surface on the sample coated with Parylene – C (Fig. 20), while the sample coated with Parylene – N revealed fibrils bundled together with various heights (Fig. 21).

The angles at the tip of the bundled fibrils are measured for the Parylene – N sample on the SEM image and on AFM profile lines.

The statistics are presented in Table 1.

The frequencies of the angles are depicted by the histogram in Figure 22.

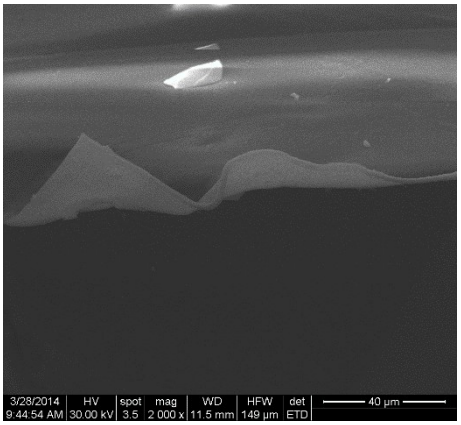

Fig. 20 - SEM parylene – C / *Suprafața parilenei-C prin microscopie cu baleiaj.*

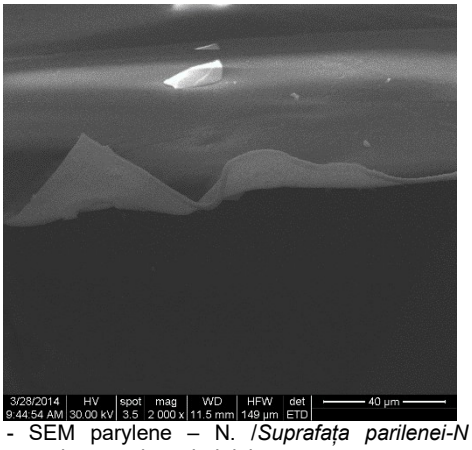

Fig. 21 - SEM parylene – N. /*Suprafața parilenei-N prin microscopie cu baleiaj.*

Table 1

Statistic results on measured angles / *Rezultate statistice pentru unghiurile măsurate.*

Statistical parameter *Parametru statistic*	Angles measured on AFM profile lines *Unghiuri măsurate prin microscopia cu forță atomică – a se vedea Fig. 22*	Angles measured on SEM images *Unghiuri măsurate prin microscopia cu baleiaj – a se vedea Fig. 22*
Mean	18.221	9.326
Standard Error	0.949	0.257
Median	15.517	9.124
Mode	13.548	#N/A
Standard Deviation	7.709	3.212
Sample Variance	59.434	10.314
Kurtosis	2.177	0.858
Skewness	1.567	0.809
Range	36.083	17.177
Minimum	6.753	3.454
Maximum	42.836	20.631
Sum	1202.594	1454.835
Count	66	156

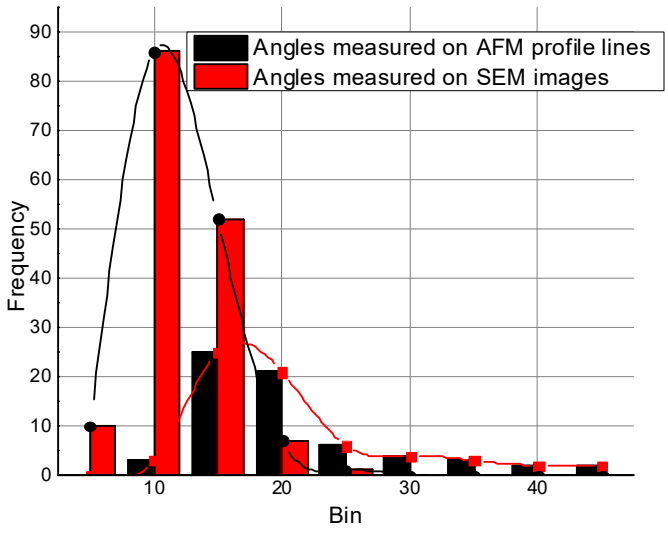

Fig. 22 - Histogram depicting measured angles on AFM profile line and SEM images / *Histograma unghiurilor măsurate prin microscopie cu forță atomică și cu baleiaj.*

Both distribution have a positive skewness, the kurtosis is higher when the angles were measured on AFM profile lines.

On the SEM images was also found that bundles of fibrils with low angles at the tip tend to bond together to form a bundle with an angle approximately equal to the sum of the angles of the individual bundles.

4. Conclusion

The measured thickness for both Parylene-N and Parylene-C at the end of the deposition process matched the thickness determined by ellipsometry

By AFM analysis a smoother surface for Parylene – C was proven, while the Parylene – N showed a dimpled surface with isolated valleys.

The SEM images on Parylene – C revealed a smooth surface, with debris, while the Parylene – N showed a dimpled surface with fibrils bundled together.

Angle measurements revealed that, usually 2 bundles of fibrils tend to bind together and form a larger bundle, with an angle at the tip almost equal to the sum of the angles of the individual bundles.

Angles measured on AFM profile lines are larger when compared to angles measured on SEM images because of the broadening effect in AFM due to tip size. Still, global features are kept similar.

The Parylene – C coating appears with a convex shape, the edges being thicker with a gradient towards the center. Parylene – N appears uniform in thickness with the dimpled aspect observed on the smaller observed surface.

At least at this scale, by surface morphology, we could infer that Parylene – N was deposited homogeneous or that the Parylene – C coating was warped. If this is so we think that Parylene-N's higher level molecular activity during deposition generates greater penetration into crevices than that observed in parylene-C, making it superior for coating complex topographies specially for medical instrumentation.

REFERENCES

1. S. Haeberle and Zengerle R Microfluidic platforms for lab-on-chip applications Lab on Chip 2007, **7**(9), 1094.
2. http://www.paryleneengineering.com/basics_of_parylene.html
3. M A Ionescu, C Ionescu and I Ciucă Scanning electron microscopy, atomic force microscopy and spectroscopic ellipsometry on Parylene-N and Parylene-C thin films deposited onto Si(111) – unpublished paper.
4. http://en.wikipedia.org/wiki/File:Di-p-xylylene.svg
5. G-R. Yahg, S. Ganguli, J. Karcz, W. N. Gill, T-M. Lu, Journal of Crystal Growth 1998, 138, 385.
6. M. A. Ionescu, C. Ionescu and I. Ciuca Polymer vapour deposition of Parylene-N and Parylene-C on Si(111). Thin film characterization by FTIR and ellipsometry. Rev. Chim. 2014, 65 (10).

****

MANIFESTĂRI ȘTIINȚIFICE / SCIENTIFIC EVENTS

The TACT 2017 will cover a wide spectrum of aspects related to thin film and coating technologies for sustainable energy, semiconductor, optoelectronic, tribological, organic, biological, protective, and functional coatings.

The TACT 2017 features **seven important symposia, one short course**, **two plenary**, and **eight keynote** talks, namely:

A. Coatings for sustainable energy
B. Nanostructured and nanocomposite coatings
C. Optical, semiconductor and optoelectronic films
D. Tribological and protective coatings
E. Organic and biological coatings
F. Metallic and magnetic coatings
G. Topical symposium: theory, simulation, and modeling; quantitative surface analysis
SC. Short course: basic principles of XPS and peak-analysis (fitting) of real-data

Contact: http://tact2017.conf.tw/site/page.aspx?pid=901&sid=1130&lang=en

****